Lis1 is an initiation factor for dynein-driven organelle transport

Martin J. Egan, Kaeling Tan, and Samara L. Reck-Peterson

Department of Cell Biology, Harvard Medical School, Boston, MA 02115

The molecular motor cytoplasmic dynein is responsible for most minus-end–directed, microtubule-based transport in eukaryotic cells. It is especially important in neurons, where defects in microtubule-based motility have been linked to neurological diseases. For example, lissencephaly is caused by mutations in the dynein-associated protein Lis1. In this paper, using the long, highly polarized hyphae of the filamentous fungus *Aspergillus nidulans*, we show that three morphologically and functionally distinct dynein cargos showed transport defects in the genetic absence of Lis1/*nudF*, raising the possibility that Lis1 is ubiquitously used for dynein-based transport. Surprisingly, both dynein and its cargo moved at normal speeds in the absence of Lis1 but with reduced frequency. Moreover, Lis1, unlike dynein and dynactin, was absent from moving dynein cargos, further suggesting that Lis1 is not required for dynein-based cargo motility once it has commenced. Based on these observations, we propose that Lis1 has a general role in initiating dynein-driven motility.

Introduction

Bidirectional transport of proteins, organelles, and mRNAs along cytosolic microtubules is essential for many aspects of eukaryotic cell biology such as cell growth, cell migration, and cell–cell communication. In humans, subtle defects in the motors responsible for these movements cause neurodevelopmental and neurodegenerative diseases, highlighting the importance of microtubule-based transport in long cells such as neurons (Hirokawa et al., 2010). Most kinesin motors move toward the microtubule plus end or toward the cell periphery (anterograde motion), whereas the dynein motor moves toward the microtubule minus end or toward the nucleus (retrograde motion). Interestingly, in humans and many other eukaryotes, there are multiple cargo-transporting kinesins (15 in humans) but only a single dynein motor gene responsible for most cytoplasmic cargo transport (Vale, 2003). Thus, a critical challenge for understanding dynein-based motility is to understand how dynein is regulated to transport diverse cargos.

The dynein motor holoenzyme is large and complex (at least eight polypeptides weighing >1.2 megadaltons), and many additional proteins and protein complexes, including the dynactin complex, Lis1, and Nudel, act as regulatory factors (Kardon and Vale, 2009; Vallee et al., 2012). Lis1 was first identified as a gene mutated in type I lissencephaly, a brain developmental disease characterized by malformations of the cerebral cortex (Reiner et al., 1993). Lis1 was later linked to dynein motor function through genetic studies in *Aspergillus nidulans*, which demonstrated that Lis1/*nudF*, like dynein/*nudA*, was required for normal nuclear distribution (Xiang et al., 1995).

Lis1's role in the dynein-mediated positioning of nuclei and centrosomes is well documented (Xiang et al., 1995; Faulkner et al., 2000; Dujardin et al., 2003; Lee et al., 2003; Cockell et al., 2004; Tanaka et al., 2004; Levy and Holzbaur, 2006; Vallee and Tsai, 2006; Tsai et al., 2007; Youn et al., 2009), but its role in the transport of other dynein cargos remains less clear. Several studies have shown that reducing Lis1 expression leads to defects in the distribution or transport of endosomes, Golgi, and lysosomes (Liu et al., 2000; Smith et al., 2000; Lenz et al., 2006; Ding et al., 2009; Lam et al., 2010; Zhang et al., 2010; Yi et al., 2011). In contrast, overexpression of Lis1 in mammalian tissue culture cells does not appear to affect organelle transport while affecting other dynein-mediated processes, leading to the conclusion that Lis1 is not required for the transport of some dynein cargos (Faulkner et al., 2000; Dujardin et al., 2003; Tsai et al., 2007). The role of Lis1 in organelle transport may also depend on the size of the organelle as well as the cell type being studied (Pandey and Smith, 2011;

Correspondence to Samara L. Reck-Peterson: reck-peterson@hms.harvard.edu

The Rockefeller University Press $30.00
J. Cell Biol. Vol. 197 No. 7 971–982
www.jcb.org/cgi/doi/10.1083/jcb.201112101

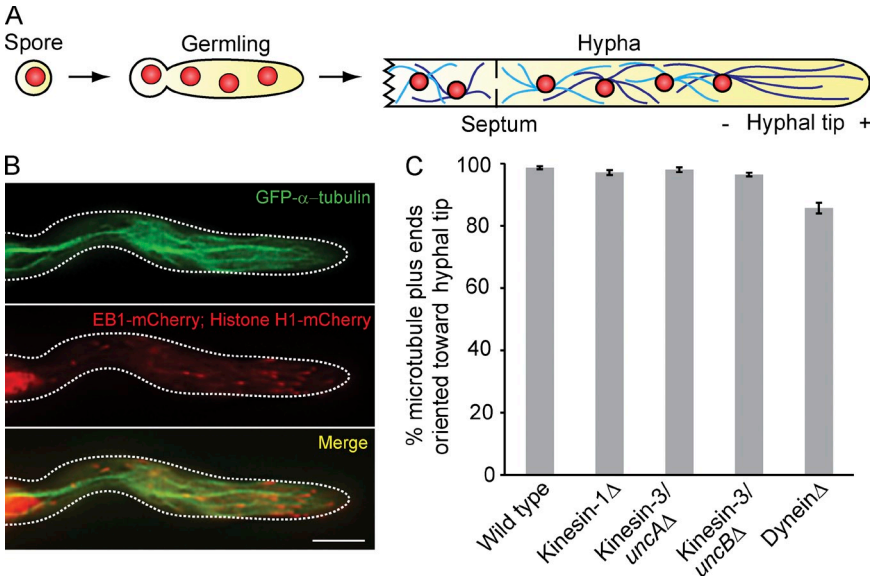

Figure 1. **Microtubules are unidirectional from the last nucleus to the hyphal tip.** (A) Cartoon depicting the development of a uninucleate *A. nidulans* spore into a mature multinucleate (in red) hypha, containing unidirectional microtubule arrays (in light and dark blue) from the last nucleus to the growing tip. Microtubule polarity is indicated by plus and minus symbols. (B) Microtubule plus ends are polarized toward the hyphal tip in wild-type hyphae. Microtubules are visualized with GFP–α-tubulin (top), microtubule plus ends with EB1-mCherry, and nuclei with histone H1–mCherry (middle). The bottom image is a merged image of the top and middle images. Dashed lines indicate the outline of the hyphae. Bar, 5 µm. (C) Bar graph showing the percentage of microtubules (±SEM) with plus ends oriented toward the hyphal tip. Only microtubules between the hyphal tip and the most proximal nucleus were analyzed. For each strain, >60 independent hyphae and >700 EB1 comets were analyzed.

Yi et al., 2011). Thus, the breadth of dynein activities in which Lis1 participates is controversial.

How Lis1 modulates dynein function is also unclear. Recently, it was proposed that Lis1 might be specifically required for dynein functions that require pulling against high loads (McKenney et al., 2010). The finding in cultured primary neurons that large cargos were more reliant on Lis1 than smaller cargos provided additional support for this idea (Pandey and Smith, 2011; Yi et al., 2011). Although several studies have shown that Lis1 can alter dynein's mechanochemical functions (Mesngon et al., 2006; Yamada et al., 2008; McKenney et al., 2010; Torisawa et al., 2011), it remains unknown whether Lis1 associates with dynein on moving cargo in vivo. In fact, in *Saccharomyces cerevisiae*, one of the most well-studied model systems for the role of Lis1 in the dynein pathway, Lis1 does not appear to interact with cargo-bound dynein (Lee et al., 2003; Markus et al., 2011). In yeast, Lis1/Pac1 is required for targeting dynein to the microtubule plus end, where it is proposed to facilitate the off-loading of dynein onto the cortex (Lee et al., 2003; Sheeman et al., 2003). Cortically positioned dynein is then thought to pull on nucleus-attached astral microtubules, biasing the movement of the daughter nucleus through the bud neck (Moore et al., 2009). Thus, the absence of cortical Lis1, but the clear presence of dynein and dynactin from cytological studies (Markus and Lee, 2011; Markus et al., 2011), suggests that Lis1 has a role in targeting and/or initiating dynein-based transport in *S. cerevisiae* but may not be required for subsequent motility.

Some of the controversy over Lis1's function comes from the variety of methods used to alter Lis1 gene expression or protein activity. Here, we have turned to the model filamentous fungus *A. nidulans*, which has several major advantages. First, unlike *S. cerevisiae*, which lacks cargo-transporting kinesins (defined here as kinesin-1, -2, and -3) and uses dynein only for nuclear positioning, *A. nidulans* uses microtubule-based transport to move components required for rapid growth of its long hyphae (Horio and Oakley, 2005; Horio, 2007). Microtubule-based motors in the *A. nidulans* genome are encoded by a single dynein gene (*nudA*) and 11 kinesin genes representing nine classes of kinesin motors (Rischitor et al., 2004). Three of these kinesins, KinA (kinesin-1 or conventional kinesin), UncA (a kinesin-3), and UncB (also a kinesin-3), are expected to be cytoplasmic cargo-transporting kinesins (Requena et al., 2001; Zekert and Fischer, 2009; Verhey et al., 2011). Here, we will refer to the dynein heavy chain gene, *nudA*, as dynein, *kinA* as kinesin-1, and *uncA* and *uncB* as kinesin-3s. Second, the subunit compositions of dynein and dynactin in *A. nidulans* are similar to their mammalian counterparts, with known homologs of almost every subunit present in the *A. nidulans* genome. Third, unlike mammalian tissue culture models, genes can easily be knocked out or modified at the endogenous loci in *A. nidulans* haploid spores (Nayak et al., 2006). Finally, given the ease of genetic manipulations in *A. nidulans* and recent advances in whole genome sequencing, in the future, *A. nidulans* will be an ideal model for performing screens to identify components required for microtubule-based transport, which has not been possible in *S. cerevisiae* because yeast do not use microtubules for long-distance organelle transport.

Here, we set out to determine whether Lis1 is required for the motility or distribution of multiple dynein cargos and whether Lis1 regulates moving cargo-bound dynein. We begin by confirming and building on previous work showing that *A. nidulans* is a robust model system for performing a comprehensive analysis of multiple microtubule-based cargos (Abenza et al., 2009; Zekert and Fischer, 2009; Zhang et al., 2010, 2011). We then show that Lis1 is required for the transport of three functionally and morphologically distinct cargos, raising the possibility that Lis1 is required for the motility of most dynein cargos. We find that although the frequency of cargo transport is decreased in the genetic absence of Lis1, the velocities of both cargo and dynein are largely unaffected, providing evidence that Lis1 is not required during motility in vivo. In further support of this, we show that Lis1 is not stably associated with moving, dynein-driven cargo, whereas both dynein and dynactin are. Based on these findings, we propose that Lis1 has a general role in the initiation of dynein-based cargo motility.

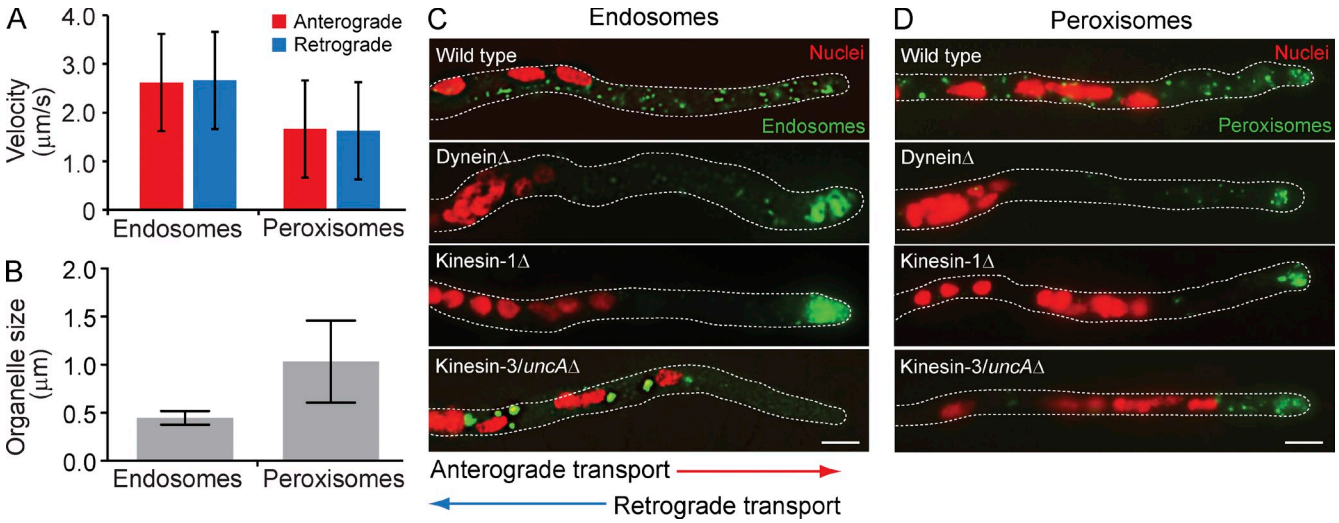

Figure 2. **Endosomes, peroxisomes, and nuclei are cargos of dynein and kinesin-3.** (A) Bar graphs showing the mean velocities of anterograde- and retrograde-moving endosomes and peroxisomes in wild-type hyphae. Endosomes moved with mean anterograde and retrograde velocities of 2.62 ± 0.83 μm/s (SD) and 2.66 ± 0.77 μm/s, respectively (n = 250). Peroxisomes moved with mean anterograde and retrograde velocities of 1.66 ± 0.77 μm/s (n = 50) and 1.63 ± 0.87 μm/s (n = 48), respectively. (B) Bar graph showing the mean sizes of endosomes and peroxisomes in wild-type hyphae. Organelles were measured along their longest axes. Typical endosomes were round, with a mean diameter of 0.45 ± 0.07 μm (SD), whereas peroxisomes were more elongated, with a mean length of 1.03 ± 0.43 μm (n = 200 for both endosomes and peroxisomes). Endosomes were statistically smaller than peroxisomes (unpaired t test, $P < 0.0001$). (C and D) Localization of GFP-Rab5/RabA–labeled endosomes, Pex11/PexK-GFP–labeled peroxisomes, and histone H1–mCherry-labeled nuclei after targeted deletion of cargo-transporting motors. Loss of the dynein heavy chain gene resulted in hyphal tip accumulation of both endosomes and peroxisomes and failure of nuclei to distribute properly. In kinesin-1Δ strains, both endosomes and peroxisomes accumulated at the hyphal tip; a slight nuclear misdistribution phenotype was also observed. Deletion of kinesin-3 did not affect nuclei distribution but caused accumulation of endosomes near nuclei and accumulation of peroxisomes in the growing hyphal tip and subapical region. Dashed lines indicate the outline of the hyphae. Bars, 5 μm.

Results

The study of microtubule-based transport has a long history in *A. nidulans* (Osmani and Mirabito, 2004), but recent advances now permit tagging or deleting motors and motor regulatory subunits with ease at their endogenous genomic loci (Nayak et al., 2006). Using these tools in combination with high-resolution microscopy, here, we systematically analyzed the regulation of microtubule-based bidirectional transport in *A. nidulans* and investigated the role of the dynein regulator Lis1 in the transport of multiple cargos.

Microtubules are unidirectional in the tips of *A. nidulans* hyphae

In *A. nidulans*, hyphal compartments contain multiple nuclei in a linear arrangement (Fig. 1 A). To examine the polarity of microtubules in hyphae, we generated a strain in which α-tubulin was tagged with GFP (Szewczyk and Oakley, 2011) and the microtubule plus-end–tracking protein EB1/*AN2862* was tagged with mCherry (Fig. 1 B). We found that 98.7 ± 0.5% (SEM) of microtubules between the hyphal tip and the most proximal nucleus were polarized with their plus ends oriented toward the growing hyphal tip (Fig. 1 C), consistent with a previous study using the plus-end marker CENP-E/KipA (Konzack et al., 2005). To determine whether microtubules remain polarized in the absence of cargo-transporting motors, we deleted dynein, kinesin-1, kinesin-3/*uncA*, or kinesin-3/*uncB* from the GFP–α-tubulin, EB1-mCherry–tagged strain. We found that the vast majority of microtubules displayed normal polarity in all motor deletion strains (Fig. 1 C). Thus, the unidirectional array of microtubules within the hyphal tip makes *A. nidulans* an ideal model system for studying bidirectional microtubule-based transport in a highly polarized cell type.

Identification of dynein and kinesin cargos in *A. nidulans*

Next, we confirmed and extended previous studies by identifying organelles that rely on microtubule-based motors for movement and distribution in *A. nidulans*. Previous studies identified endosomal (Abenza et al., 2009) and nuclear (Xiang et al., 1994) distribution along hyphae as dependent on microtubule-based motors. Here, we visualized and also quantified endosome motility in the hyphal tip, using an N-terminal GFP tag on Rab5/RabA to specifically label early endosomes (Abenza et al., 2009). Endosomes moved bidirectionally along the cell length (Video 1), with comparable velocities in the anterograde and retrograde directions (2.62 ± 0.83 μm/s [mean ± SD] vs. 2.66 ± 0.77 μm/s, respectively; Fig. 2 A).

To identify additional organelles dependent on microtubules for motility, we next characterized the motile behavior of peroxisomes by labeling them with a GFP tag on the peroxisomal membrane protein Pex11/PexK (Hynes et al., 2008). We found that peroxisomes, like endosomes, displayed both anterograde and retrograde movements (Video 2). Peroxisomes were significantly larger than endosomes (Fig. 2 B) and traveled with mean anterograde and retrograde velocities of 1.66 ± 0.77 and 1.63 ± 0.87 μm/s (mean ± SD; Fig. 2 A), respectively. Thus, for a given organelle, anterograde and retrograde speeds of transport are similar, but endosomes are significantly smaller in size and move more rapidly than peroxisomes ($P < 0.0001$, using unpaired t-tests).

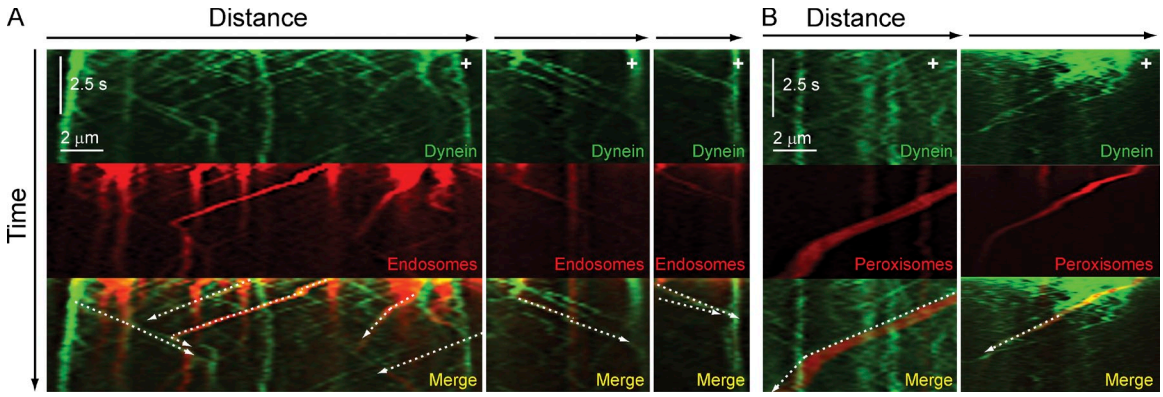

Figure 3. **Endosomes and peroxisomes colocalize with moving dynein.** (A and B) Kymographs were generated from time-lapse videos. Dynein-3xGFP (top) colocalizes with mCherry-Rab5/RabA–labeled endosomes (A) and mCherry-PTS1–labeled peroxisomes (B; middle) in wild-type hyphae. Bottom images show merged images with white dashed arrows highlighting examples of colocalized events. The locations of microtubule plus ends in the hyphal tip are indicated by white plus signs.

To identify the motors required for the distribution and transport of these dynamic organelles, we individually deleted the genes encoding each cargo-transporting, microtubule-based motor present in the *A. nidulans* genome in strains expressing labeled endosomes, peroxisomes, and nuclei. Consistent with prior studies, we found that nuclei were not distributed properly in strains lacking either dynein or kinesin-1 (Fig. 2, C and D; Xiang et al., 1994; Zhang et al., 2003). Loss of kinesin-1 likely perturbs nuclear positioning as a result of mislocalization of dynein (Zhang et al., 2003); here, we confirmed that most dynein plus-end localization is lost in the absence of kinesin-1 (Fig. S1). Unlike kinesin-1, neither kinesin-3 gene (*uncA* or *uncB*) was required for nuclear positioning or dynein plus-end localization (Figs. 2 [C and D], S1, and S2 [A and B]). Thus, we have confirmed and broadened previous studies by showing that of all cargo-transporting kinesins, only kinesin-1 is required for nuclear positioning and dynein plus-end localization.

Next, we tested which microtubule-based motors were responsible for endosome and peroxisome transport. In strains lacking the dynein heavy chain gene, both endosomes and peroxisomes accumulated in the hyphal tip and were nonmotile, suggesting that dynein is responsible for the retrograde movement of these organelles (Fig. 2 [C and D] and Video 3; Abenza et al., 2009; Zhang et al., 2010). In strains lacking kinesin-1, similar to those lacking dynein, both peroxisomes and endosomes accumulated in the hyphal tip (Fig. 2, C and D), likely reflecting kinesin-1's role in localizing dynein to the microtubule plus end (Fig. S1; Zhang et al., 2003).

Interestingly, although not required for nuclear distribution, deletion of kinesin-3/*uncA* caused defects in endosome and peroxisome distribution and motility (Fig. 2, C and D). In kinesin-3/*uncAΔ* hyphae, endosomes accumulated in small patches near nuclei (Fig. 2 C), whereas peroxisomes accumulated aberrantly in the tip region (Fig. 2 D). As was observed in dyneinΔ hyphae, endosomes and peroxisomes were immotile in kinesin-3/*uncAΔ* hyphae (Video 4). The only other cargo-transporting kinesin present in the *A. nidulans* genome, kinesin-3/*uncB*, was not required for the transport of either peroxisomes or endosomes (Fig. S2, A and B). Thus, for both endosomes and peroxisomes in *A. nidulans*, dynein and kinesin-3/UncA are the opposite polarity motors responsible for bidirectional transport.

Our observation that deletion of either dynein or kinesin-3/*uncA* perturbed organelle transport in both the retrograde and anterograde directions suggests some type of interdependence between plus- and minus-end–directed motors present on a shared cargo. Interdependence of bidirectional microtubule-based transport has been observed in many eukaryotic organisms (recent examples include Gross et al. [2003], Lenz et al. [2006], Barkus et al. [2008], Ally et al. [2009], Uchida et al. [2009], and Encalada et al. [2011]). To examine this further, we C-terminally tagged kinesin-3/UncA with GFP and examined its motile behavior in wild-type and dyneinΔ hyphae (Fig. S3). In wild-type hyphae, kinesin-3/UncA-GFP particles moved bidirectionally in a manner reminiscent of endosome movements (Fig. S3 A). However, in strains lacking dynein, although we detected rare anterograde-directed movements (Fig. S3 C), kinesin-3/UncA-GFP predominantly accumulated at the hyphal tip, consistent with attachment to organellar cargo (Fig. S3, B and C). Our findings suggest that in the absence of dynein, kinesin-3/UncA–mediated anterograde transport is perturbed as a result of sequestration of kinesin-3/UncA at the microtubule plus end. We propose that kinesin-3/UncA may require dynein to recycle back to the microtubule minus end.

Dynein colocalizes with moving endosomes and peroxisomes

The lack of endosome and peroxisome motility in strains lacking dynein suggests that dynein directly transports these organelles. If this were the case, dynein should colocalize with retrograde-moving endosomes and peroxisomes. To determine the localizations of dynein and its putative cargo, we tagged the endogenous dynein heavy chain with three tandem copies of GFP (3xGFP) at its C terminus. Importantly, addition of the 3xGFP tag did not disrupt dynein function, as the strain grew similarly to wild-type strains and did not share the slow growth phenotype exhibited by *nud* (nuclear distribution) mutants (Fig. S4, A and B). Endosome and peroxisome cargo were visualized with mCherry-Rab5/RabA and mCherry-PTS1 (peroxisome

targeting signal 1), respectively. Analysis of kymographs made from time-lapse videos of these dynein and organelle-colabeled strains demonstrated the presence of discrete dynein runs that colocalized with retrograde-moving endosomes (Fig. 3 A) or peroxisomes (Fig. 3 B). Interestingly, we also observed dynein colocalization with endosomes moving toward the microtubule plus end (Fig. 3 A), suggesting that dynein is a passenger on kinesin-3/UncA–driven, anterograde-moving endosomes. These data suggest that dynein directly drives the retrograde motility of endosomes and peroxisomes within the hyphal tip.

In summary, these experiments along with other work in the field show that nuclear distribution requires dynein and kinesin-1 (which localizes dynein) but not kinesin-3s, whereas endosome and peroxisome transport requires dynein, kinesin-1 (to localize dynein), and kinesin-3/UncA but not kinesin-3/UncB. Next, we turned our focus to the role of the dynein regulator Lis1 in the distribution and transport of nuclei, endosomes, and peroxisomes.

Lis1 is required for the distribution of endosomes and peroxisomes

In *Aspergillus*, Lis1/*nudF*, referred to here as Lis1, is required for the migration of nuclei along rapidly growing hyphae (Xiang et al., 1995) and has more recently been implicated in the transport of Rab5/RabA-marked early endosomes (Zhang et al., 2010). Here, we sought to confirm and further characterize Lis1's role in endosome transport and additionally to determine whether Lis1 was required for the dynein-mediated trafficking of peroxisomes. We deleted the sole endogenous copy of Lis1 from a strain with GFP-Rab5/RabA–marked endosomes and mCherry-PTS1–marked peroxisomes. Lis1Δ hyphae displayed severe defects in both endosome (Fig. 4 A) and peroxisome (Fig. 4 B) distributions. Both classes of organelle clustered at the hyphal tip, similar to defects observed in dyneinΔ hyphae (Fig. 2, A and B). Kymographs from time-lapse videos of labeled endosomes and peroxisomes indicated that these organelles were largely immotile (Fig. 4, A and B), with defects in both anterograde and retrograde motility. Thus, Lis1 is required for the proper distribution of three morphologically and functionally distinct dynein-dependent cargos: nuclei, endosomes, and peroxisomes.

Lis1 is not essential for endosome or dynein motility in vivo

Although the majority of endosomes were immotile in Lis1Δ hyphae (Fig. 4 A), we did observe occasional bidirectional movements of endosomes (Fig. 4 C). To further examine this, we calculated the velocity of bidirectional endosome movements in the absence of Lis1. To study the process with high resolution and detail, we chose to focus on endosomes, which are significantly more dynamic than peroxisomes. Strikingly, we found that there was very little change in the velocities of anterograde (Fig. 4 D) and retrograde (Fig. 4 E) endosome movements in the absence of Lis1. The presence of occasional organelles that move at normal speeds in the complete genetic absence of Lis1 raises the possibility that Lis1 is not essential for dynein-driven endosome movements.

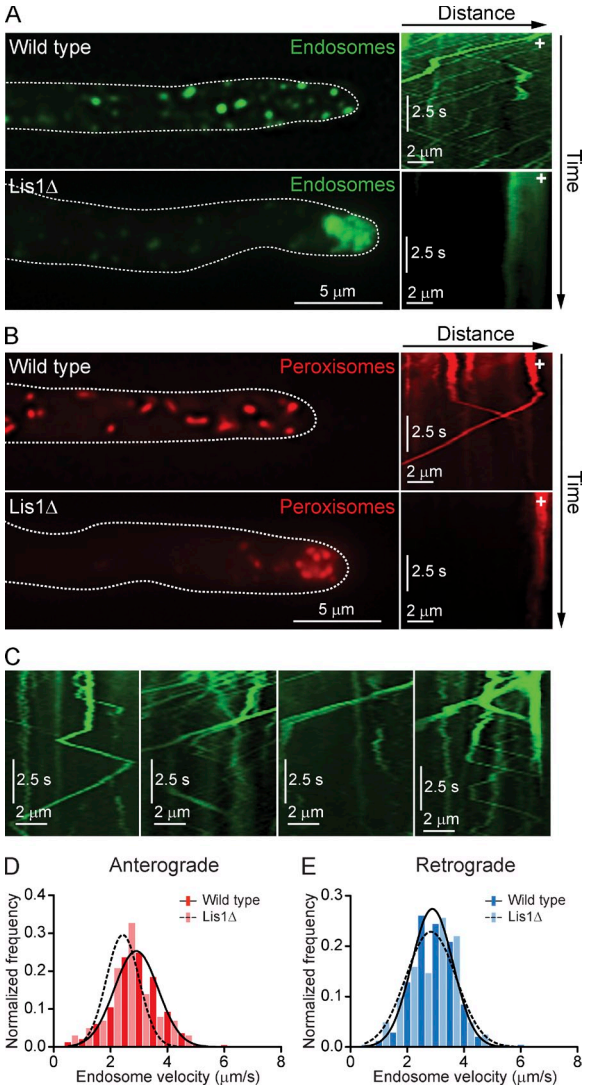

Figure 4. **Lis1 is required for the distribution of peroxisomes and endosomes but is not essential for endosome motility in vivo.** (A and B) In wild-type hyphae, GFP-Rab5/RabA–labeled endosomes (A) and mCherry-PTS1–labeled peroxisomes (B) are uniformly distributed (left images) and move bidirectionally, as shown in kymographs generated from time-lapse videos (right images). In Lis1Δ hyphae, endosomes (A) and peroxisomes (B) mislocalize to the hyphal tip (left images) and are largely immotile (right images). Dashed lines indicate the outline of the hyphae. The locations of microtubule plus ends in the hyphal tip are indicated by white plus signs. (C) Kymographs of GFP-labeled endosomes in Lis1Δ mutants show examples of Lis1-independent movements of endosomes. (D) Histograms of velocities of anterograde-directed endosomes from wild-type versus Lis1Δ strains. Mean velocities are 2.62 ± 0.83 µm/s (SD) in wild-type hyphae and 2.25 ± 0.85 µm/s in Lis1Δ hyphae ($P = 0.0002$; $n = 250$ [wild type]; $n = 101$ [Lis1Δ]). (E) Histogram of velocities of retrograde-directed endosomes from wild-type versus Lis1Δ strains. Mean velocities are 2.66 ± 0.77 µm/s (SD) in wild-type hyphae and 2.43 ± 0.81 µm/s in Lis1Δ hyphae ($P = 0.0169$; $n = 250$ [wild type]; $n = 82$ [Lis1Δ]).

Our finding that endosomal cargo in Lis1Δ hyphae can move at relatively normal speeds suggested to us that dynein motility itself may not require Lis1 in vivo. To test this directly, we monitored dynein movement in Lis1Δ hyphae. Significantly, dynein-3xGFP was detected moving both toward and away from microtubule plus ends in Lis1Δ hyphae (Fig. 5 A and Video 5). Notably, the mean dynein particle velocity in either

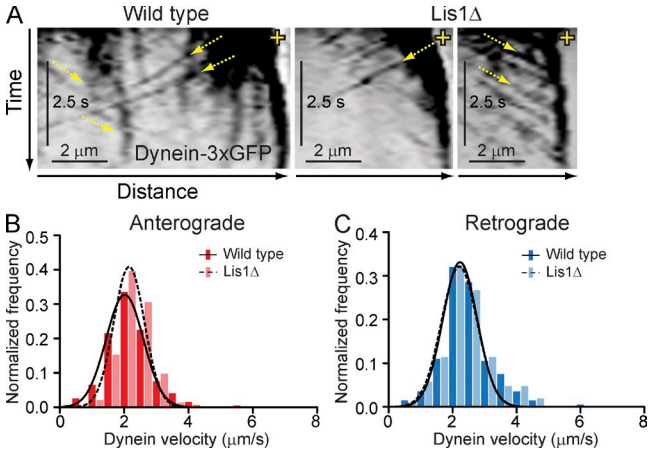

Figure 5. **Lis1 is not required for dynein motility.** (A) Kymographs of dynein-3xGFP particles reveal movements toward and away from the microtubule plus end in both wild-type and Lis1Δ hyphae. Yellow dashed arrows indicate discrete particle movements toward and away from the hyphal tip. The locations of microtubule plus ends in the hyphal tip are indicated by yellow plus signs. (B) Histograms showing anterograde velocities of dynein-3xGFP particles in wild-type and Lis1Δ hyphae. Mean velocities are 2.09 ± 0.70 μm/s (SD) in wild-type and 2.17 ± 0.52 μm/s in Lis1Δ hyphae (P = 0.197; *n* = 200 [wild type]; *n* = 144 [Lis1Δ]). (C) Histograms showing retrograde velocities of dynein-3xGFP particles in wild-type and Lis1Δ hyphae. Mean velocities are 2.38 ± 0.80 μm/s (SD) in wild-type and 2.30 ± 0.75 μm/s in Lis1Δ hyphae (P = 0.420, *n* = 200 [wild type]; *n* = 105 [Lis1Δ]).

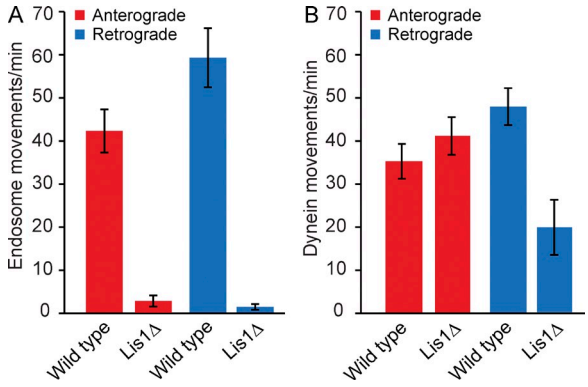

Figure 6. **The frequencies of organelle and dynein movements are decreased in the absence of Lis1.** (A) Bar graph of anterograde and retrograde endosome flux in wild-type and Lis1Δ hyphae. Rates were calculated from the number of endosomes that crossed a line drawn perpendicular to and 10 μm away from the hyphal tip during 3 min of observation. For wild-type hyphae, 127 vesicles moved in the anterograde direction, and 177 vesicles moved in the retrograde direction. For Lis1Δ hyphae, eight vesicles moved in the anterograde direction, and five vesicles moved in the retrograde direction. Error bars represent SD. (B) Bar graph of the rate at which dynein particles enter and leave microtubule plus ends in wild-type and Lis1Δ hyphae. The frequency of anterograde particle movements in Lis1Δ hyphae was not significantly different from that of the wild-type strain (41 ± 4 per minute [SEM] vs. 35 ± 4 per minute, respectively; P = 0.357). The frequency of retrograde dynein particle movements in the absence of Lis1 was significantly lower than that of the wild-type strain (20 ± 6 per minute vs. 48 ± 4 per minute, respectively; P = 0.005; *n* = 347 [wild type]; *n* = 142 [Lis1Δ]).

the anterograde (Fig. 5 B) or retrograde (Fig. 5 C) direction was not affected by deleting Lis1. Thus, Lis1 is not essential for the movement of either dynein or its cargo in vivo but is still necessary for proper cargo distribution along hyphae.

Lis1 increases the frequency of endosome and dynein movements

In the absence of Lis1, endosomes and peroxisomes accumulate at hyphal tips, and retrograde movements are quite rare despite dynein's relatively normal capacity for motility, raising the possibility that Lis1 is required for initiating dynein-driven cargo transport. To test this, we first calculated the frequency of endosome movements by determining the number of anterograde and retrograde events that crossed a defined region within the hyphal tip during a fixed time interval. In wild-type hyphae, the frequencies of anterograde and retrograde endosome movements were 42 ± 5 per minute (SEM) and 59 ± 7 per minute, respectively (Fig. 6 A), whereas in Lis1Δ hyphae, the frequencies decreased dramatically to 3 ± 1 per minute (anterograde) and 2 ± 1 per minute (retrograde; Fig. 6 A). In contrast, we observed no bidirectional movements in hyphae lacking either dynein (Video 3) or the dynactin subunit p150/*nudM* (Fig. S5 A).

We also analyzed the frequency of dynein movements by counting the number of particles that arrive at or depart from the microtubule plus end over a given time period. The frequency of dynein particle anterograde movements in Lis1Δ hyphae was not significantly different from those in the wild-type strain (Fig. 6 B). However, the frequency of retrograde dynein particle movements in Lis1Δ hyphae was significantly lower than that of the wild-type strain (Fig. 6 B). Interestingly, in contrast to Lis1, deletion of the dynactin subunit p150/*nudM* completely abolished all dynein movement (Fig. S5 B). Our findings that the genetic absence of Lis1 does not markedly alter dynein and endosome velocities but does reduce the frequency of their movements are consistent with the hypothesis that Lis1 is necessary for initiating dynein-driven cargo transport but not for subsequent dynein motor function to transport endosomes away from the hyphal tip. In contrast, dynactin appears to be essential for the motility of both dynein and its cargo in vivo.

Lis1 is not stably associated with dynein cargo

If the primary role of Lis1 in dynein-dependent transport were during initiation of this process, Lis1 may not remain stably associated with cargo after transport commences. To test this hypothesis, we generated a strain expressing both Lis1-GFP and mCherry-Rab5/RabA–labeled endosomes. Importantly, the addition of GFP to the C terminus of Lis1 did not disrupt Lis1 function, as this strain grew at wild-type rates (Fig. S4, A and C). Lis1-GFP localized to the plus ends of microtubules and was largely immotile (Fig. 7 A and Video 6). Although we did observe occasional retrograde-moving Lis1-GFP particles, their movements were very short in length and only very rarely colocalized with a moving endosome. To quantify this observation, we determined the percentage of moving endosomes that colocalized with either dynein or Lis1 and found that 93.4 ± 3.0% (mean ± SEM; *n* = 110) of moving endosomes colocalized with a dynein-3xGFP particle, whereas only 1.8 ± 1.0% (*n* = 148) of endosomes colocalized with a Lis1-GFP particle (Fig. 7 B). To ensure that the absence of Lis1 on moving endosomes was not a result of imaging limitations, we tagged the

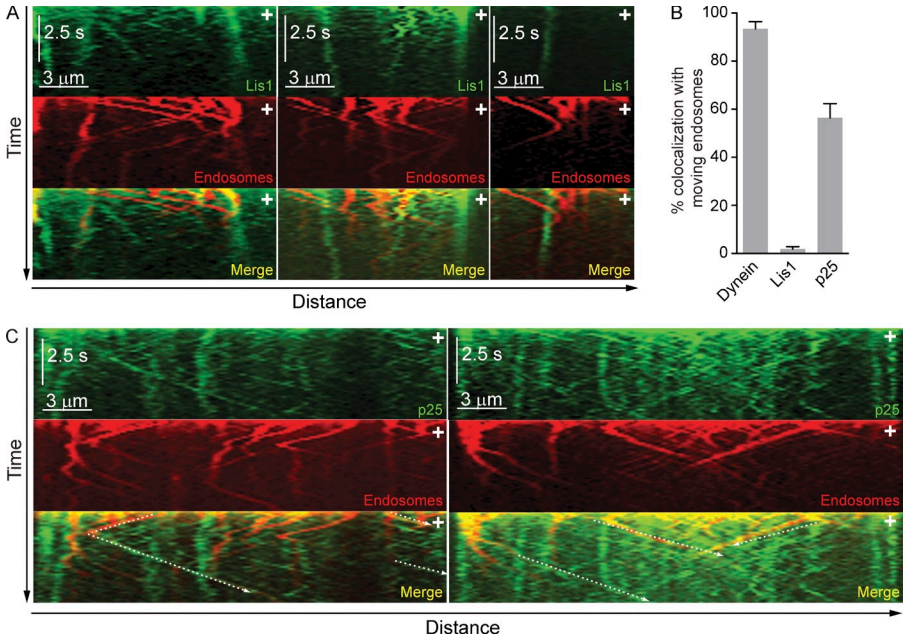

Figure 7. **Lis1 is not stably associated with moving dynein cargos.** (A) Kymographs of Lis1-GFP (top) and mCherry-Rab5/RabA endosomes (middle) in *A. nidulans* germlings. Bottom images are merged images of the top and middle images. (B) Bar graph of the percentage of endosomes colocalizing with dynein, Lis1, or dynactin. 93.4 ± 3.0% (SEM) of moving mCherry-Rab5/RabA endosomes colocalized with a dynein-3xGFP particle (n = 110 endosomes). 1.8 ± 1.0% of endosomes colocalized with a Lis1-GFP particle (n = 148 endosomes). 56.4 ± 5.9% of endosomes colocalized with a p25-GFP particle (n = 161 endosomes). (C) Kymographs of p25-GFP (top) and mCherry-Rab5/RabA endosomes (middle) in *A. nidulans* germlings. Frequent colocalization of p25-GFP and endosomes was observed. Bottom images are merged images of the top and middle images. The locations of microtubule plus ends in the hyphal tip are indicated by white plus signs. White dashed arrows highlight examples of colocalized events.

dynactin subunit p25 with a single GFP at its C terminus and generated a strain expressing both p25-GFP and mCherry-Rab5/RabA–labeled endosomes (Fig. 7 C). Unlike Lis1-GFP, p25-GFP was highly motile and associated with 56.4 ± 5.9% of moving endosomes (mean ± SEM; n = 161; Fig. 7 B). In these experiments, because each dynein dimer contains six GFPs, each Lis1 dimer contains two GFPs, and each dynactin complex has only a single GFP on its p25 subunit (Eckley et al., 1999), we have likely underestimated the number of endosomes that colocalize with p25 and Lis1. In summary, these results show that the majority of retrograde endosome movements are associated with dynein and dynactin but not Lis1.

We hypothesized that Lis1 could be required during transport initiation for proper loading of dynein onto its cargo. In Lis1Δ hyphae, but not wild-type hyphae, endosomes and peroxisomes accumulate aberrantly at hyphal tips (Fig. 4, A and B). If Lis1 were dispensable for loading dynein onto cargo, we expected that dynein would accumulate on these mislocalized cargos, as previously proposed (Zhang et al., 2010). To test this idea, we visualized the extent of colocalization between dynein-3xGFP and endosomes (Fig. 8, A and B) or peroxisomes (Fig. 8, C and D) in wild-type and Lis1Δ hyphae. Although we observed increased dynein-3xGFP signal in Lis1Δ hyphal tips, this signal did not colocalize with either endosomes (Fig. 8 B) or peroxisomes (Fig. 8 D) in Lis1Δ hyphae, supporting the idea that Lis1 is required for loading dynein onto its cellular cargos at the microtubule plus end.

Discussion

Here, we have undertaken a comprehensive study of the role of Lis1 in dynein-based organelle transport. We analyzed the dynamics of both dynein and its cargos in the polarized haploid hyphae of *A. nidulans* strains lacking the single endogenous copy of the Lis1 gene. We found that Lis1 is required for the proper distribution of three functionally and morphologically distinct dynein cargos, including both small cargo (endosomes) and larger cargo (peroxisomes and nuclei). To gain insight into which stages of the dynein pathway Lis1 acts, we analyzed the frequency and velocity of endosome and dynein motions in the absence of Lis1. Surprisingly, we found that both endosomes and dynein moved at relatively normal speeds in the complete absence of Lis1 but with reduced frequency. Moreover, Lis1, unlike dynein and dynactin, is absent from nearly all moving dynein cargos, further supporting our finding that Lis1 is not strictly required for dynein-based cargo motility once movement has commenced. Based on these observations, we propose that Lis1 has a general role in the initiation of dynein-driven motility.

Many dynein cargos require Lis1

Despite a large number of studies in diverse biological systems, the mechanistic role of Lis1 in the transport of dynein cargos remains controversial. To clearly interpret the function of Lis1 in the transport of dynein cargos, we genetically deleted the sole copy of the endogenous Lis1 gene in *A. nidulans*. Many prior studies in mammalian cells or the fungus *Ustilago maydis* have relied on methods that lead to incomplete depletion of either the Lis1 mRNA or protein (Faulkner et al., 2000; Tai et al., 2002; Dujardin et al., 2003; Lenz et al., 2006; Ding et al., 2009; Lam et al., 2010; Pandey and Smith, 2011; Yi et al., 2011). Our finding that Lis1 is required for the proper distribution of endosomes, peroxisomes, and nuclei leads us to propose that most, if not all, dynein cargo will require Lis1 function. Consistent with our observations, decreases in Lis1 expression have been shown to cause defects in axonal transport (Liu et al., 2000) and distribution of endosomes, lysosomes, and Golgi (Liu et al., 2000; Lenz et al., 2006; Ding et al., 2009; Lam et al., 2010; Pandey and Smith, 2011; Yi et al., 2011), as well as nuclear migration and centrosome positioning (Xiang et al., 1995; Faulkner et al., 2000; Dujardin et al., 2003; Lee et al., 2003; Sheeman et al.,

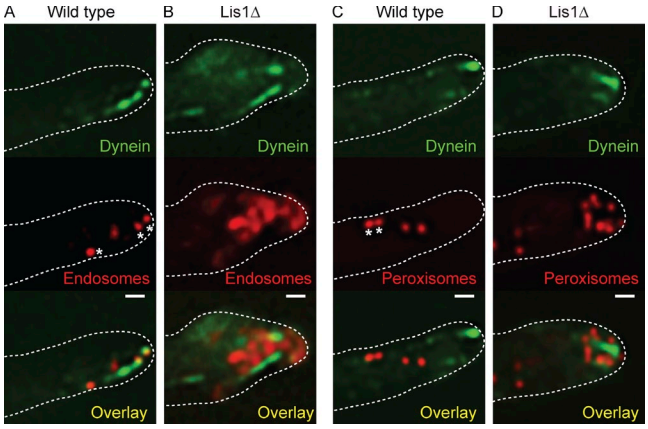

Figure 8. **In the absence of Lis1, dynein fails to colocalize with endosomes or peroxisomes at the hyphal tip.** (A–D) Micrographs of the extreme tips of wild-type (A and C) and Lis1Δ (B and D) hyphae expressing dynein-3xGFP and mCherry-Rab5/RabA–labeled endosomes (A and B) or mCherry-PTS1–labeled peroxisomes (C and D). In wild-type hyphae, endosomes (A) and peroxisomes (C) localize along the length of microtubules, labeled by dynein-3xGFP, which decorates the microtubule plus ends and localizes to discrete puncta. Dynein-3xGFP colocalized with moving endosomes and peroxisomes (labeled with white asterisks in A and C), as determined by kymograph analysis. In Lis1Δ hyphae, dynein-3xGFP localizes to comets at the microtubule plus ends and to the cytoplasm (B and D, top) but does not colocalize with either endosomes (B, bottom) or peroxisomes (D, bottom) accumulated at the hyphal tip. Dashed lines indicate the outline of the hyphae. Bars, 1 µm.

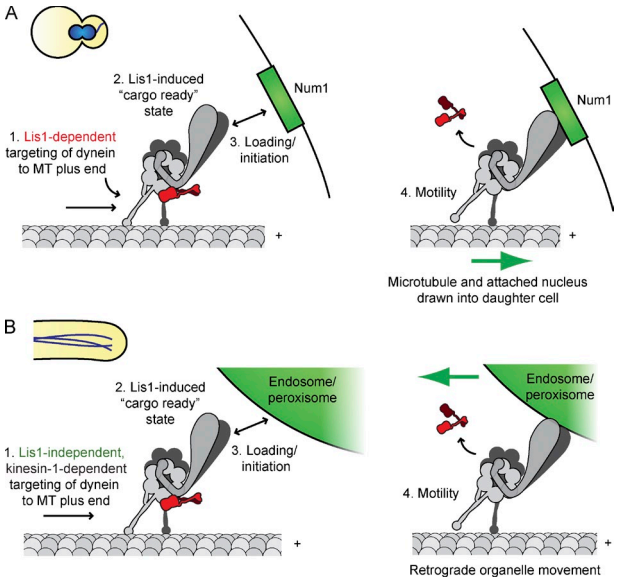

Figure 9. **Model of Lis1 function in *S. cerevisiae* and *A. nidulans*.** (A) In *S. cerevisiae*, Lis1 (red) is required to recruit dynein (gray) to microtubule plus ends (step 1). Lis1 binding to dynein anchors dynein at the plus end and induces a cargo-ready conformation (step 2). Dynein is then off-loaded to the cortical receptor Num1 (green; step 3). In the absence of Lis1, cortically anchored dynein walks toward the microtubule minus end, biasing movement of the microtubule-attached nucleus into the daughter cell (step 4, green arrow). (B) In *A. nidulans* hyphae, dynein (gray) is targeted to the microtubule plus end in a Lis1-independent (red), kinesin-1–dependent manner (step 1). Lis1 binding to dynein anchors dynein at the plus end and induces a cargo-ready conformation (step 2). Dynein then binds to endosomes or peroxisomes (green; step 3). In the absence of Lis1, organelle-associated dynein drives retrograde endosome or peroxisome motility (step 4, green arrow).

2003; Cockell et al., 2004; Tanaka et al., 2004; Tsai et al., 2007; Levy and Holzbaur, 2008; Youn et al., 2009).

Only a handful of studies have reported Lis1-independent dynein-based processes. First, experiments in which Lis1 or Lis1 fragments were overexpressed in mammalian tissue culture cells did not reveal any defects in the transport of lysosomes or Golgi but did show that other dynein-dependent mitotic processes were disrupted (Faulkner et al., 2000; Dujardin et al., 2003; Tsai et al., 2007). This is in contrast to RNAi depletion of Lis1 (also in cultured mammalian cells), which perturbs the distributions of Golgi, lysosomes, and late endosomes (Lam et al., 2010). One possible explanation for these differences is that Lis1 overexpression does not fully disrupt all of Lis1's function, whereas depletion of Lis1 does. Notably, several studies suggest that Lis1 function is highly dose dependent (Hirotsune et al., 1998; Li et al., 2005; Bi et al., 2009; Wang and Zheng, 2011; Zyłkiewicz et al., 2011). Second, in cultured neurons, injection of a Lis1 function-blocking antibody or RNAi of Lis1 inhibited the motility of large but not small lysosomes or acidic organelles, raising the possibility that Lis1 is specifically required for high-load functions (Pandey and Smith, 2011; Yi et al., 2011). Here, in *A. nidulans* hyphae lacking the sole genomic copy of Lis1, we find no evidence for a size-dependent requirement for Lis1 function; both small endosomes and larger peroxisomes and nuclei require Lis1 for proper distribution. In filamentous fungi, internal turgor pressure directed toward the hyphal tip participates in hyphal growth (Lew, 2011), raising the possibility that dynein encounters significant opposing force while transporting cargo in the retrograde direction. However, we still observe occasional endosome movements in the absence of Lis1, indicating that Lis1 is not required to overcome any additional load imparted by turgor pressure.

A general role for Lis1 in initiating dynein-driven transport

One of the most extensive models of the cell biological function of Lis1 comes from studies of its role in *S. cerevisiae* (Fig. 9 A; Lee et al., 2003, 2005; Sheeman et al., 2003; Markus et al., 2009, 2011; Markus and Lee, 2011). In yeast, the dynein pathway is required for mitotic spindle alignment and nuclear migration (Eshel et al., 1993; Li et al., 1993). In this system, the Lis1 ortholog (also known as Pac1) is required for the targeting of dynein to the microtubule plus end, a prerequisite for off-loading the motor to a receptor, Num1, which is present on the cell cortex (Lee et al., 2003; Sheeman et al., 2003). After off-loading, cortically anchored dynein binds to cytosolic microtubules and moves toward the microtubule minus end. Because the microtubule-organizing center is embedded in the nuclear envelope of the daughter cell's nucleus, these pulling forces bias the movement of the daughter cell's nucleus into the daughter cell (Stuchell-Brereton et al., 2011).

Mechanistically, these results are consistent with a requirement for Lis1 to initiate but not to sustain dynein-driven motility. Because Lis1 can enhance dynein's microtubule affinity (Yamada et al., 2008; McKenney et al., 2010), it may assist in

concentrating dynein at the microtubule plus end before cortical offloading. Additionally, Lis1 may cause a conformational change in dynein that is a prerequisite for cargo binding (Markus et al., 2009). Because Lis1 is not stably localized to the cortex in yeast (Lee et al., 2003; Markus et al., 2011), it does not appear to be required for sustained pulling forces. Current data do not rule out the possibilities that Lis1 is briefly localized to the cortex and plays a role in assisting movements generated by cortically localized dynein or that Lis1 is only transiently associated with the cortex and thus not observable by fluorescence microscopy.

We hypothesize that in *A. nidulans*, loading of dynein onto endosomes occurs via a similar mechanism (Fig. 9 B). In support of a role for Lis1 in initiating cargo motility, we found that deletion of Lis1 decreases the frequency of endosome and dynein movements but does not dramatically alter the speeds of these movements. Additionally, we showed that dynein and dynactin were stably present on moving endosomes, but Lis1 was not. In our model for Lis1 function in *A. nidulans* organellar transport, dynein first arrives at the microtubule plus end in a Lis1-independent, kinesin-1–dependent manner (Fig. 9 B, step 1; Zhang et al., 2003). Next, we propose that binding of Lis1 biases dynein to a microtubule-engaged state at the microtubule plus end, perhaps inducing a conformational change in dynein (Fig. 9 B, step 2) that promotes cargo binding (Fig. 9 B, step 3). After dynein is loaded onto cargo, motility proceeds without stably bound Lis1 (Fig. 9 B, step 4). It is possible that binding of dynactin to dynein triggers the movement of dynein away from the microtubule plus end, as a recent study found that NudE (a Lis1 binding partner) and dynactin compete for interaction with the dynein intermediate chain (McKenney et al., 2011). Here, we observed stable association of dynein and dynactin but not Lis1 with moving endosomes. As is the case in yeast, we cannot exclude the possibility that Lis1 is transiently associated with endosome-bound dynein and plays some further role in the commencement of cargo movement or during cargo motility. Overall, our results support a role for Lis1 in initiating dynein-based cargo transport.

Interestingly, we find that dynein or Lis1 deletion reduces the frequency of both anterograde and retrograde transport of endosomes. As described in the Results section, such interdependence of bidirectional transport has been observed in many eukaryotic organisms. Anterograde transport of endosomes in *Aspergillus* is mediated by kinesin-3/UncA. Our ability to observe only rare kinesin3/UncA movements in the absence of dynein suggests that kinesin3/UncA requires dynein for recycling back to the microtubule minus end. Based on our cargo initiation model, we interpret the loss of anterograde motility in the absence of dynein or Lis1 as being a direct consequence of loss of Lis1-dependent initiation of retrograde motility, which would be required for kinesin3/UncA recycling.

Materials and methods

Fungal growth conditions

A. nidulans strains were grown in yeast extract and glucose medium (Szewczyk et al., 2006) or minimal medium (Nayak et al., 2010), supplemented with 1 mg/ml uracil, 2.4 mg/ml uridine, 2.5 µg/ml riboflavin, 1 µg/ml para-aminobenzoic acid, and 0.5 µg/ml pyridoxine when required. Expression from the *alcA* promoter was induced by replacing glucose with 0.1% fructose. Glufosinate was used at a final concentration of 25 µl/ml (Nayak et al., 2010).

Strain construction

A. nidulans strains used in this study are listed in Table S1. Strains containing deletions of kinesin-1/*kinA*, kinesin-3/*uncA*, kinesin-3/*uncB*, dynein/*nudA*, and Lis1/*nudF* were created by homologous recombination to replace the endogenous gene with *AfpyrG* (*Aspergillus fumigatus pyrG*), *Afpyro* (*Aspergillus fumigatus pyro*), or *bar* (Straubinger et al., 1992) as selectable markers (Szewczyk et al., 2006). The *nudA::AfpyrG* and *nudF::AfpyrG* deletion cassettes were provided by S. Osmani (Ohio State University, Columbus, OH), J. Dunlap (Dartmouth Medical School, Hanover, NH), and the Fungal Genetics Stock Center. Gene deletions were verified by Southern blot or PCR analyses using genomic DNA isolated, as previously described (Lee and Taylor, 1990).

Constructs to delete genes or tag endogenous genes with TagGFP2 (*A. nidulans* codon optimized; Subach et al., 2008), GFP, 3xGFP, or mCherry were generated using fusion PCR (Szewczyk et al., 2006) or yeast homologous recombination (Orr-Weaver et al., 1983) and integrated at the endogenous locus using homologous recombination in strains lacking *ku70* (Nayak et al., 2006). Tagged strains were confirmed by PCR. Some strains were created through genetic crosses, as previously described (Todd et al., 2007).

Live-cell fluorescence microscopy

For live-cell imaging of mature hyphae, spores were inoculated on minimal medium plates containing the appropriate auxotrophic supplements and grown at 37°C for 12–24 h. Colonies were excised from plates as agar squares, inverted onto 10 µl of liquid minimal medium in an eight-chambered chamber (Lab-Tek; Thermo Fisher Scientific) or a 35-mm FluoroDish (World Precision Instruments, Inc.) and observed at 22°C. For live-cell imaging of germlings, spores were resuspended in 0.01% Tween 80 solution. The spore suspension was diluted at 1:1,000 in liquid minimal medium containing appropriate auxotrophic supplements. The spore and media mix (3 ml) was added to a 35-mm FluoroDish and incubated at 22°C for 15–20 h before imaging.

Wide-field fluorescence images were collected at 22°C using a Plan-Apochromat 100×/1.40 oil objective (Nikon) on an epifluorescence microscope (Ti; Nikon) with the Perfect Focus System (Nikon) and a charge-coupled device camera (ORCA-ER; Hamamatsu Photonics), all controlled by Elements software (Nikon). Simultaneous multicolor wide-field images were collected at 22°C using a custom-built microscope (DeltaVision OMX; Applied Precision) equipped with a Plan-Apochromat N 60×/1.12 oil objective lens (Olympus). GFP and mCherry were simultaneously excited using 488- and 592.5-nm laser lines. A series of dichroic mirrors in the OMX light path (Standard Filter Set v2; Applied Precision) was used to split the emission light from the two fluorophores to two different cooled charge-coupled device cameras (CoolSNAP HQ2; Photometrics). A narrow-band emission filter in front of each camera was used to select appropriate wavelengths (525/20 and 615/24 for GFP and mCherry, respectively). Images were acquired using DeltaVision software (v2.23) and deconvolved using softWoRx image processing software (v4.50; Applied Precision) using the enhanced ratio method. Brightness and contrast adjustments to images were subsequently made using ImageJ (v1.43; National Institutes of Health) or Photoshop CS4 (v11.0.2; Adobe), and figures were compiled in Illustrator CS4 (v. 14.0.0; Adobe).

Image and data analysis

The percentage of unidirectional microtubules in hyphal tips was determined by observing the polarity of EB1-mCherry comets. Comets with tails pointing toward the last nucleus and tips pointing toward the hyphal tip versus comets oriented in the opposite direction were scored.

For quantitative analysis of endosome velocity, we used a strain in which endosomes were marked with *A. nidulans* codon–optimized TagGFP2 (Subach et al., 2008)-Rab5/RabA. TagGFP2 is a GFP variant that is significantly brighter than GFP or EGFP (Subach et al., 2008). N-terminal GFP tagging of Rab5/RabA was previously shown to be functional (Abenza et al., 2009), and we observed no growth differences between tagging the endogenous *rabA* locus versus the *argB*-targeted *rabA* expressed under the control of the *alcA* promoter (Abenza et al., 2009).

Endosome, peroxisome, and dynein velocities were measured using ImageJ (v1.43). Maximum-intensity projections were generated from time-lapse sequences to define the trajectory of particles of interest. The segmented line tool was used to trace the trajectories and map them onto the original video sequence, which was subsequently resliced to generate a kymograph. The velocities of individual particles were calculated from the

inverse of the slopes of kymograph traces. Dynein flux measurements were calculated from kymographs generated from 10-s time-lapse sequences by counting the number of dynein-3xGFP particles entering and leaving the microtubule plus end. Microtubules were selected for analysis based on image quality and the clarity of discrete particle movements. Endosome flux was calculated as the total number of vesicles that crossed a line drawn perpendicular to and 10 µm away from the hyphal tip over 3 min.

For quantitative analysis of organelle size, endosomes and peroxisomes were measured along their longest axis using the line tool and measure function in ImageJ (v1.43). Our measurements for peroxisomes were in the range of those described in previous EM analysis of these organelles in *A. nidulans* (Valenciano et al., 1998). Our measurements for endosomes were close to the theoretical diffraction limit for our imaging conditions; thus, this number represents an upper limit for endosome size. Consistent with our analysis, EM studies of endosomes in *A. nidulans* and mammalian cells report sizes in the range of <100–500 nm (Murk et al., 2003; Griffith et al., 2011).

Data visualization and statistical analyses were performed using GraphPad Prism (5.0d; GraphPad Software), Excel (v12.3.2; Microsoft), MATLAB (MathWorks), and ImageJ (v1.43). For Figs. 4 (D and E) and 5 (B and C), the Lis1Δ histogram data were shifted 0.25 U to the right relative to the wild-type data to visualize both datasets simultaneously; the Gaussian fits of the same data were not shifted.

Online supplemental material

Fig. S1 shows that localization of dynein to microtubule plus ends requires kinesin-1 but not kinesin-3/*uncA* or kinesin-3/*uncB*. Fig. S2 shows that endosome and peroxisome transport is unaffected by deletion of kinesin-3/*uncB*. Fig. S3 shows that kinesin-3/UncA accumulates in the hyphal tip in the absence of dynein. Fig. S4 shows that tagging dynein or Lis1 with GFP does not affect function. Fig. S5 shows that dynactin is required for endosome and dynein motility. Video 1 shows GFP-Rab5/RabA–labeled endosome dynamics in a wild-type hypha. Video 2 shows Pex11/PexK-GFP–labeled peroxisome dynamics in a wild-type hypha. Video 3 shows GFP-Rab5/RabA–labeled endosome dynamics in a dyneinΔ hypha. Video 4 shows GFP-Rab5/RabA–labeled endosome dynamics in a kinesin3/*uncA*Δ hypha. Video 5 shows dynein-3xGFP dynamics in a wild-type hypha. Video 6 shows Lis1-GFP and mCherry-Rab5/RabA–labeled endosomes in a wild-type hypha. Table S1 lists the *A. nidulans* strains used in this study. Online supplemental material is available at http://www.jcb.org/cgi/content/full/jcb.201112101/DC1.

We would like to thank Michael Hynes (The University of Melbourne, Melbourne, Australia), Berl Oakley (University of Kansas, Lawrence, KS), Miguel Peñalva (Centro de Investigaciones Biologicas CSIC, Madrid, Spain), and Xin Xiang (Uniformed Services University, Bethesda, MD) for strains, reagents, and protocols; Stephen Osmani, Jay Dunlap, and the Fungal Genetics Stock Center for deletion cassettes; Michael Wu and Natalie Heer for help generating strains and reagents; Anthony Roberts, Julie Huang, Mark McClintock, and Xin Xiang for comments on the manuscript; Gaudenz Danuser and Applied Precision for use of the custom-built DeltaVision OMX microscope; and the Nikon Imaging Center at Harvard Medical School for their support.

S.L. Reck-Peterson is funded by the Rita Allen Foundation, the Armenise-Harvard Foundation, and a National Institutes of Health New Innovator award (1 DP2 OD004268-01).

Submitted: 19 December 2011
Accepted: 16 May 2012

References

Abenza, J.F., A. Pantazopoulou, J.M. Rodríguez, A. Galindo, and M.A. Peñalva. 2009. Long-distance movement of *Aspergillus nidulans* early endosomes on microtubule tracks. *Traffic*. 10:57–75. http://dx.doi.org/10.1111/j.1600-0854.2008.00848.x

Ally, S., A.G. Larson, K. Barlan, S.E. Rice, and V.I. Gelfand. 2009. Opposite-polarity motors activate one another to trigger cargo transport in live cells. *J. Cell Biol.* 187:1071–1082. http://dx.doi.org/10.1083/jcb.200908075

Barkus, R.V., O. Klyachko, D. Horiuchi, B.J. Dickson, and W.M. Saxton. 2008. Identification of an axonal kinesin-3 motor for fast anterograde vesicle transport that facilitates retrograde transport of neuropeptides. *Mol. Biol. Cell*. 19:274–283. http://dx.doi.org/10.1091/mbc.E07-03-0261

Bi, W., T. Sapir, O.A. Shchelochkov, F. Zhang, M.A. Withers, J.V. Hunter, T. Levy, V. Shinder, D.A. Peiffer, K.L. Gunderson, et al. 2009. Increased LIS1 expression affects human and mouse brain development. *Nat. Genet.* 41:168–177. http://dx.doi.org/10.1038/ng.302

Cockell, M.M., K. Baumer, and P. Gönczy. 2004. lis-1 is required for dynein-dependent cell division processes in *C. elegans* embryos. *J. Cell Sci.* 117:4571–4582. http://dx.doi.org/10.1242/jcs.01344

Ding, C., X. Liang, L. Ma, X. Yuan, and X. Zhu. 2009. Opposing effects of Ndel1 and alpha1 or alpha2 on cytoplasmic dynein through competitive binding to Lis1. *J. Cell Sci.* 122:2820–2827. http://dx.doi.org/10.1242/jcs.048777

Dujardin, D.L., L.E. Barnhart, S.A. Stehman, E.R. Gomes, G.G. Gundersen, and R.B. Vallee. 2003. A role for cytoplasmic dynein and LIS1 in directed cell movement. *J. Cell Biol.* 163:1205–1211. http://dx.doi.org/10.1083/jcb.200310097

Eckley, D.M., S.R. Gill, K.A. Melkonian, J.B. Bingham, H.V. Goodson, J.E. Heuser, and T.A. Schroer. 1999. Analysis of dynactin subcomplexes reveals a novel actin-related protein associated with the arp1 minifilament pointed end. *J. Cell Biol.* 147:307–320. http://dx.doi.org/10.1083/jcb.147.2.307

Encalada, S.E., L. Szpankowski, C.H. Xia, and L.S. Goldstein. 2011. Stable kinesin and dynein assemblies drive the axonal transport of mammalian prion protein vesicles. *Cell*. 144:551–565. http://dx.doi.org/10.1016/j.cell.2011.01.021

Eshel, D., L.A. Urrestarazu, S. Vissers, J.C. Jauniaux, J.C. van Vliet-Reedijk, R.J. Planta, and I.R. Gibbons. 1993. Cytoplasmic dynein is required for normal nuclear segregation in yeast. *Proc. Natl. Acad. Sci. USA*. 90:11172–11176. http://dx.doi.org/10.1073/pnas.90.23.11172

Faulkner, N.E., D.L. Dujardin, C.Y. Tai, K.T. Vaughan, C.B. O'Connell, Y. Wang, and R.B. Vallee. 2000. A role for the lissencephaly gene LIS1 in mitosis and cytoplasmic dynein function. *Nat. Cell Biol.* 2:784–791. http://dx.doi.org/10.1038/35041020

Griffith, J., M.A. Peñalva, and F. Reggiori. 2011. Adaptation of the Tokuyasu method for the ultrastructural study and immunogold labelling of filamentous fungi. *J. Electron Microsc. (Tokyo)*. 60:211–216. http://dx.doi.org/10.1093/jmicro/dfr026

Gross, S.P., Y. Guo, J.E. Martinez, and M.A. Welte. 2003. A determinant for directionality of organelle transport in *Drosophila* embryos. *Curr. Biol.* 13:1660–1668. http://dx.doi.org/10.1016/j.cub.2003.08.032

Hirokawa, N., S. Niwa, and Y. Tanaka. 2010. Molecular motors in neurons: Transport mechanisms and roles in brain function, development, and disease. *Neuron*. 68:610–638. http://dx.doi.org/10.1016/j.neuron.2010.09.039

Hirotsune, S., M.W. Fleck, M.J. Gambello, G.J. Bix, A. Chen, G.D. Clark, D.H. Ledbetter, C.J. McBain, and A. Wynshaw-Boris. 1998. Graded reduction of Pafah1b1 (Lis1) activity results in neuronal migration defects and early embryonic lethality. *Nat. Genet.* 19:333–339. http://dx.doi.org/10.1038/1221

Horio, T. 2007. Role of microtubules in tip growth of fungi. *J. Plant Res.* 120:53–60. http://dx.doi.org/10.1007/s10265-006-0043-2

Horio, T., and B.R. Oakley. 2005. The role of microtubules in rapid hyphal tip growth of *Aspergillus nidulans*. *Mol. Biol. Cell*. 16:918–926. http://dx.doi.org/10.1091/mbc.E04-09-0798

Hynes, M.J., S.L. Murray, G.S. Khew, and M.A. Davis. 2008. Genetic analysis of the role of peroxisomes in the utilization of acetate and fatty acids in *Aspergillus nidulans*. *Genetics*. 178:1355–1369. http://dx.doi.org/10.1534/genetics.107.085795

Kardon, J.R., and R.D. Vale. 2009. Regulators of the cytoplasmic dynein motor. *Nat. Rev. Mol. Cell Biol.* 10:854–865. http://dx.doi.org/10.1038/nrm2804

Konzack, S., P.E. Rischitor, C. Enke, and R. Fischer. 2005. The role of the kinesin motor KipA in microtubule organization and polarized growth of *Aspergillus nidulans*. *Mol. Biol. Cell*. 16:497–506. http://dx.doi.org/10.1091/mbc.E04-02-0083

Lam, C., M.A. Vergnolle, L. Thorpe, P.G. Woodman, and V.J. Allan. 2010. Functional interplay between LIS1, NDE1 and NDEL1 in dynein-dependent organelle positioning. *J. Cell Sci.* 123:202–212. http://dx.doi.org/10.1242/jcs.059337

Lee, S.B., and J.W. Taylor. 1990. Isolation of DNA from fungal mycelia and single spores. *In* PCR Protocols: A Guide to Methods and Applications. D.G.M. Innis, J. Sninsky, and T. White, editors. Academic Press, Orlando, Florida. 282–287.

Lee, W.L., J.R. Oberle, and J.A. Cooper. 2003. The role of the lissencephaly protein Pac1 during nuclear migration in budding yeast. *J. Cell Biol.* 160:355–364. http://dx.doi.org/10.1083/jcb.200209022

Lee, W.L., M.A. Kaiser, and J.A. Cooper. 2005. The offloading model for dynein function: Differential function of motor subunits. *J. Cell Biol.* 168:201–207. http://dx.doi.org/10.1083/jcb.200407036

Lenz, J.H., I. Schuchardt, A. Straube, and G. Steinberg. 2006. A dynein loading zone for retrograde endosome motility at microtubule plus-ends. *EMBO J.* 25:2275–2286. http://dx.doi.org/10.1038/sj.emboj.7601119

Levy, J.R., and E.L. Holzbaur. 2006. Cytoplasmic dynein/dynactin function and dysfunction in motor neurons. *Int. J. Dev. Neurosci.* 24:103–111. http://dx.doi.org/10.1016/j.ijdevneu.2005.11.013

Levy, J.R., and E.L. Holzbaur. 2008. Dynein drives nuclear rotation during forward progression of motile fibroblasts. *J. Cell Sci.* 121:3187–3195. http://dx.doi.org/10.1242/jcs.033878

Lew, R.R. 2011. How does a hypha grow? The biophysics of pressurized growth in fungi. *Nat. Rev. Microbiol.* 9:509–518. http://dx.doi.org/10.1038/nrmicro2591

Li, J., W.L. Lee, and J.A. Cooper. 2005. NudEL targets dynein to microtubule ends through LIS1. *Nat. Cell Biol.* 7:686–690. http://dx.doi.org/10.1038/ncb1273

Li, Y.Y., E. Yeh, T. Hays, and K. Bloom. 1993. Disruption of mitotic spindle orientation in a yeast dynein mutant. *Proc. Natl. Acad. Sci. USA*. 90:10096–10100. http://dx.doi.org/10.1073/pnas.90.21.10096

Liu, Z., R. Steward, and L. Luo. 2000. *Drosophila* Lis1 is required for neuroblast proliferation, dendritic elaboration and axonal transport. *Nat. Cell Biol.* 2:776–783. http://dx.doi.org/10.1038/35041011

Markus, S.M., and W.L. Lee. 2011. Regulated offloading of cytoplasmic dynein from microtubule plus ends to the cortex. *Dev. Cell*. 20:639–651. http://dx.doi.org/10.1016/j.devcel.2011.04.011

Markus, S.M., J.J. Punch, and W.L. Lee. 2009. Motor- and tail-dependent targeting of dynein to microtubule plus ends and the cell cortex. *Curr. Biol.* 19:196–205. http://dx.doi.org/10.1016/j.cub.2008.12.047

Markus, S.M., K.M. Plevock, B.J. St Germain, J.J. Punch, C.W. Meaden, and W.L. Lee. 2011. Quantitative analysis of Pac1/LIS1-mediated dynein targeting: Implications for regulation of dynein activity in budding yeast. *Cytoskeleton (Hoboken)*. 68:157–174. http://dx.doi.org/10.1002/cm.20502

McKenney, R.J., M. Vershinin, A. Kunwar, R.B. Vallee, and S.P. Gross. 2010. LIS1 and NudE induce a persistent dynein force-producing state. *Cell*. 141:304–314. http://dx.doi.org/10.1016/j.cell.2010.02.035

McKenney, R.J., S.J. Weil, J. Scherer, and R.B. Vallee. 2011. Mutually exclusive cytoplasmic dynein regulation by NudE-Lis1 and dynactin. *J. Biol. Chem.* 286:39615–39622. http://dx.doi.org/10.1074/jbc.M111.289017

Mesngon, M.T., C. Tarricone, S. Hebbar, A.M. Guillotte, E.W. Schmitt, L. Lanier, A. Musacchio, S.J. King, and D.S. Smith. 2006. Regulation of cytoplasmic dynein ATPase by Lis1. *J. Neurosci.* 26:2132–2139. http://dx.doi.org/10.1523/JNEUROSCI.5095-05.2006

Moore, J.K., M.D. Stuchell-Brereton, and J.A. Cooper. 2009. Function of dynein in budding yeast: Mitotic spindle positioning in a polarized cell. *Cell Motil. Cytoskeleton*. 66:546–555. http://dx.doi.org/10.1002/cm.20364

Murk, J.L., G. Posthuma, A.J. Koster, H.J. Geuze, A.J. Verkleij, M.J. Kleijmeer, and B.M. Humbel. 2003. Influence of aldehyde fixation on the morphology of endosomes and lysosomes: Quantitative analysis and electron tomography. *J. Microsc.* 212:81–90. http://dx.doi.org/10.1046/j.1365-2818.2003.01238.x

Nayak, T., E. Szewczyk, C.E. Oakley, A. Osmani, L. Ukil, S.L. Murray, M.J. Hynes, S.A. Osmani, and B.R. Oakley. 2006. A versatile and efficient gene-targeting system for *Aspergillus nidulans*. *Genetics*. 172:1557–1566. http://dx.doi.org/10.1534/genetics.105.052563

Nayak, T., H. Edgerton-Morgan, T. Horio, Y. Xiong, C.P. De Souza, S.A. Osmani, and B.R. Oakley. 2010. γ-Tubulin regulates the anaphase-promoting complex/cyclosome during interphase. *J. Cell Biol.* 190:317–330. http://dx.doi.org/10.1083/jcb.201002105

Orr-Weaver, T.L., J.W. Szostak, and R.J. Rothstein. 1983. Genetic applications of yeast transformation with linear and gapped plasmids. *Methods Enzymol.* 101:228–245. http://dx.doi.org/10.1016/0076-6879(83)01017-4

Osmani, S.A., and P.M. Mirabito. 2004. The early impact of genetics on our understanding of cell cycle regulation in *Aspergillus nidulans*. *Fungal Genet. Biol.* 41:401–410. http://dx.doi.org/10.1016/j.fgb.2003.11.009

Pandey, J.P., and D.S. Smith. 2011. A Cdk5-dependent switch regulates Lis1/Ndel1/dynein-driven organelle transport in adult axons. *J. Neurosci.* 31:17207–17219. http://dx.doi.org/10.1523/JNEUROSCI.4108-11.2011

Reiner, O., R. Carrozzo, Y. Shen, M. Wehnert, F. Faustinella, W.B. Dobyns, C.T. Caskey, and D.H. Ledbetter. 1993. Isolation of a Miller-Dieker lissencephaly gene containing G protein beta-subunit-like repeats. *Nature*. 364:717–721. http://dx.doi.org/10.1038/364717a0

Requena, N., C. Alberti-Segui, E. Winzenburg, C. Horn, M. Schliwa, P. Philippsen, R. Liese, and R. Fischer. 2001. Genetic evidence for a microtubule-destabilizing effect of conventional kinesin and analysis of its consequences for the control of nuclear distribution in *Aspergillus nidulans*. *Mol. Microbiol.* 42:121–132. http://dx.doi.org/10.1046/j.1365-2958.2001.02609.x

Rischitor, P.E., S. Konzack, and R. Fischer. 2004. The Kip3-like kinesin KipB moves along microtubules and determines spindle position during synchronized mitoses in *Aspergillus nidulans* hyphae. *Eukaryot. Cell*. 3:632–645. http://dx.doi.org/10.1128/EC.3.3.632-645.2004

Sheeman, B., P. Carvalho, I. Sagot, J. Geiser, D. Kho, M.A. Hoyt, and D. Pellman. 2003. Determinants of *S. cerevisiae* dynein localization and activation: Implications for the mechanism of spindle positioning. *Curr. Biol.* 13:364–372. http://dx.doi.org/10.1016/S0960-9822(03)00013-7

Smith, D.S., M. Niethammer, R. Ayala, Y. Zhou, M.J. Gambello, A. Wynshaw-Boris, and L.H. Tsai. 2000. Regulation of cytoplasmic dynein behaviour and microtubule organization by mammalian Lis1. *Nat. Cell Biol.* 2:767–775. http://dx.doi.org/10.1038/35041000

Straubinger, B., E. Straubinger, S. Wirsel, G. Turgeon, and O.C. Yoder. 1992. Versitile fungal transformation vectors carrying the selectable marker bar gene of *Streptomyces hygroscopicus*. *Fungal Genet. Newsl.* 39:82–83.

Stuchell-Brereton, M.D., J.K. Moore, and J.A. Cooper. 2011. The role of dynein in yeast nuclear segregation. *In* Handbook of Dynein. Pan Stanford Publishing Pte. Ltd., Singapore. 325–362.

Subach, O.M., I.S. Gundorov, M. Yoshimura, F.V. Subach, J. Zhang, D. Grüenwald, E.A. Souslova, D.M. Chudakov, and V.V. Verkhusha. 2008. Conversion of red fluorescent protein into a bright blue probe. *Chem. Biol.* 15:1116–1124. http://dx.doi.org/10.1016/j.chembiol.2008.08.006

Szewczyk, E., and B.R. Oakley. 2011. Microtubule dynamics in mitosis in *Aspergillus nidulans*. *Fungal Genet. Biol.* 48:998–999. http://dx.doi.org/10.1016/j.fgb.2011.07.003

Szewczyk, E., T. Nayak, C.E. Oakley, H. Edgerton, Y. Xiong, N. Taheri-Talesh, S.A. Osmani, and B.R. Oakley. 2006. Fusion PCR and gene targeting in *Aspergillus nidulans*. *Nat. Protoc.* 1:3111–3120. (published erratum appears in *Nat. Protoc.* 2006. 1:31120) http://dx.doi.org/10.1038/nprot.2006.405

Tai, C.Y., D.L. Dujardin, N.E. Faulkner, and R.B. Vallee. 2002. Role of dynein, dynactin, and CLIP-170 interactions in LIS1 kinetochore function. *J. Cell Biol.* 156:959–968. http://dx.doi.org/10.1083/jcb.200109046

Tanaka, T., F.F. Serneo, C. Higgins, M.J. Gambello, A. Wynshaw-Boris, and J.G. Gleeson. 2004. Lis1 and doublecortin function with dynein to mediate coupling of the nucleus to the centrosome in neuronal migration. *J. Cell Biol.* 165:709–721. http://dx.doi.org/10.1083/jcb.200309025

Todd, R.B., M.A. Davis, and M.J. Hynes. 2007. Genetic manipulation of *Aspergillus nidulans*: Meiotic progeny for genetic analysis and strain construction. *Nat. Protoc.* 2:811–821. http://dx.doi.org/10.1038/nprot.2007.112

Torisawa, T., A. Nakayama, K. Furuta, M. Yamada, S. Hirotsune, and Y.Y. Toyoshima. 2011. Functional dissection of LIS1 and NDEL1 towards understanding the molecular mechanisms of cytoplasmic dynein regulation. *J. Biol. Chem.* 286:1959–1965. http://dx.doi.org/10.1074/jbc.M110.169847

Tsai, J.W., K.H. Bremner, and R.B. Vallee. 2007. Dual subcellular roles for LIS1 and dynein in radial neuronal migration in live brain tissue. *Nat. Neurosci.* 10:970–979. http://dx.doi.org/10.1038/nn1934

Uchida, A., N.H. Alami, and A. Brown. 2009. Tight functional coupling of kinesin-1A and dynein motors in the bidirectional transport of neurofilaments. *Mol. Biol. Cell*. 20:4997–5006. http://dx.doi.org/10.1091/mbc.E09-04-0304

Vale, R.D. 2003. The molecular motor toolbox for intracellular transport. *Cell*. 112:467–480. http://dx.doi.org/10.1016/S0092-8674(03)00111-9

Valenciano, S., J.R. De Lucas, I. Van der Klei, M. Veenhuis, and F. Laborda. 1998. Characterization of *Aspergillus nidulans* peroxisomes by immunoelectron microscopy. *Arch. Microbiol.* 170:370–376. http://dx.doi.org/10.1007/s002030050655

Vallee, R.B., and J.W. Tsai. 2006. The cellular roles of the lissencephaly gene LIS1, and what they tell us about brain development. *Genes Dev.* 20:1384–1393. http://dx.doi.org/10.1101/gad.1417206

Vallee, R.B., R.J. McKenney, and K.M. Ori-McKenney. 2012. Multiple modes of cytoplasmic dynein regulation. *Nat. Cell Biol.* 14:224–230. http://dx.doi.org/10.1038/ncb2420

Verhey, K.J., N. Kaul, and V. Soppina. 2011. Kinesin assembly and movement in cells. *Annu Rev Biophys*. 40:267–288. http://dx.doi.org/10.1146/annurev-biophys-042910-155310

Wang, S., and Y. Zheng. 2011. Identification of a novel dynein binding domain in nudel essential for spindle pole organization in *Xenopus* egg extract. *J. Biol. Chem.* 286:587–593. http://dx.doi.org/10.1074/jbc.M110.181578

Xiang, X., S.M. Beckwith, and N.R. Morris. 1994. Cytoplasmic dynein is involved in nuclear migration in *Aspergillus nidulans*. *Proc. Natl. Acad. Sci. USA*. 91:2100–2104. http://dx.doi.org/10.1073/pnas.91.6.2100

Xiang, X., A.H. Osmani, S.A. Osmani, M. Xin, and N.R. Morris. 1995. NudF, a nuclear migration gene in *Aspergillus nidulans*, is similar to the human LIS-1 gene required for neuronal migration. *Mol. Biol. Cell*. 6:297–310.

Yamada, M., S. Toba, Y. Yoshida, K. Haratani, D. Mori, Y. Yano, Y. Mimori-Kiyosue, T. Nakamura, K. Itoh, S. Fushiki, et al. 2008. LIS1 and NDEL1 coordinate the plus-end-directed transport of cytoplasmic dynein. *EMBO J.* 27:2471–2483. http://dx.doi.org/10.1038/emboj.2008.182

Yi, J.Y., K.M. Ori-McKenney, R.J. McKenney, M. Vershinin, S.P. Gross, and R.B. Vallee. 2011. High-resolution imaging reveals indirect coordination

of opposite motors and a role for LIS1 in high-load axonal transport. *J. Cell Biol.* 195:193–201. http://dx.doi.org/10.1083/jcb.201104076

Youn, Y.H., T. Pramparo, S. Hirotsune, and A. Wynshaw-Boris. 2009. Distinct dose-dependent cortical neuronal migration and neurite extension defects in Lis1 and Ndel1 mutant mice. *J. Neurosci.* 29:15520–15530. http://dx.doi.org/10.1523/JNEUROSCI.4630-09.2009

Zekert, N., and R. Fischer. 2009. The *Aspergillus nidulans* kinesin-3 UncA motor moves vesicles along a subpopulation of microtubules. *Mol. Biol. Cell*. 20:673–684. http://dx.doi.org/10.1091/mbc.E08-07-0685

Zhang, J., S. Li, R. Fischer, and X. Xiang. 2003. Accumulation of cytoplasmic dynein and dynactin at microtubule plus ends in *Aspergillus nidulans* is kinesin dependent. *Mol. Biol. Cell*. 14:1479–1488. http://dx.doi.org/10.1091/mbc.E02-08-0516

Zhang, J., L. Zhuang, Y. Lee, J.F. Abenza, M.A. Peñalva, and X. Xiang. 2010. The microtubule plus-end localization of *Aspergillus* dynein is important for dynein-early-endosome interaction but not for dynein ATPase activation. *J. Cell Sci.* 123:3596–3604. http://dx.doi.org/10.1242/jcs.075259

Zhang, J., X. Yao, L. Fischer, J.F. Abenza, M.A. Peñalva, and X. Xiang. 2011. The p25 subunit of the dynactin complex is required for dynein–early endosome interaction. *J. Cell Biol.* 193:1245–1255. http://dx.doi.org/10.1083/jcb.201011022

Zhuang, L., J. Zhang, and X. Xiang. 2007. Point mutations in the stem region and the fourth AAA domain of cytoplasmic dynein heavy chain partially suppress the phenotype of NUDF/LIS1 loss in *Aspergillus nidulans*. *Genetics*. 175:1185–1196. http://dx.doi.org/10.1534/genetics.106.069013

Zyłkiewicz, E., M. Kijańska, W.C. Choi, U. Derewenda, Z.S. Derewenda, and P.T. Stukenberg. 2011. The N-terminal coiled-coil of Ndel1 is a regulated scaffold that recruits LIS1 to dynein. *J. Cell Biol.* 192:433–445. http://dx.doi.org/10.1083/jcb.201011142